



Monitoring organic matter transformation of olive oil production residues in a full-scale composting plant by fluorescence spectroscopy

Marta P. Rueda^a, Ana Domínguez-Vidal^{a,*}, Eulogio J. Llorent-Martínez^a,
Víctor Aranda^b, María José Ayora-Cañada^a

^a Department of Physical and Analytical Chemistry, Universidad de Jaén, Campus Las Lagunillas E-23071, Jaén, Spain

^b Department of Geology, Universidad de Jaén, Campus Las Lagunillas E-23071, Jaén, Spain

ARTICLE INFO

Keywords:

Olive mill pomace compost
Compost maturity
Dissolved Organic matter
Humification
Fluorescence spectroscopy
PARAFAC

ABSTRACT

Composting wet olive mill pomace, the main by-product of two-phase centrifugation systems, is an attractive valorization strategy in the context of regenerative agriculture. A comprehensive study of the changes in fluorescence signatures during the co-composting of this residue with olive tree pruning wastes and animal manure in a full-scale composting plant was performed. This compost showed more complex features than others at the initial stages of the process, exhibiting a singular band in the synchronous spectrum (500 nm) here attributed to polyphenol-pectin interactions. PARAFAC-derived components from Excitation-Emission matrices (EEMs) of water extracts were compared with those of fractions isolated following alkaline extraction at different maturity stages. The increase with composting of the component associated with humic-like substances (Ex 225, 365 nm/Em 476 nm) was more marked in the isolated humic acid fraction than in water extracts. Thus, the predominance of fulvic-like substances in water extracts explains inconsistencies previously reported about the relevance of the humic-like component during the composting process and the extent of humification. Finally, the correlation between PARAFAC components and several compost maturity parameters was studied. The negative correlation between the protein-like component and the germination index was explained by the protein-polyphenol interactions reflected in the emission spectra of this component. A strong positive correlation between both fulvic and humic fluorescent components and cation exchange capacity was found. In general, mature compost showed $C/N \leq 20$ and no phytotoxicity (GI around 60%) although differences related to the heterogeneity of the large composting pile were important.

1. Introduction

Olive oil production generates huge quantities of mill waste in a short period, which represents a significant environmental problem in producing areas, particularly in the Mediterranean region where about 95% of worldwide olive oil is produced. In modern olive mills, the production of olive oil primarily relies on centrifugation-based continuous systems. They can be categorized into three-phase and two-phase systems, depending on the type of horizontal decanter used. In three-phase centrifugal systems, a significant

* Corresponding author.

E-mail address: adovidal@ujaen.es (A. Domínguez-Vidal).

<https://doi.org/10.1016/j.eti.2024.103695>

Received 29 February 2024; Received in revised form 9 May 2024; Accepted 25 May 2024

Available online 27 May 2024

2352-1864/© 2024 The Author(s). Published by Elsevier B.V. This is an open access article under the CC BY-NC-ND license (<http://creativecommons.org/licenses/by-nc-nd/4.0/>).

amount of water is added to the decanter to enhance the extraction of olive oil from the olive pulp. Apart from the oil extracted, two by-products are generated: olive mill wastewater and olive mill pomace (OMP), a solid waste. The two-phase centrifugation systems have been implemented in many olive mills in the last two decades as more environmentally friendly alternatives due to their reduced water consumption. These two-phase systems yield only a semisolid waste called “alperujo” or wet olive mill pomace (WOMP) which needs special attention (Roig et al., 2006). WOMP is a semisolid paste, with remnants of olive pulp and skin, and a moisture content of 55–75%. It is also highly abundant in organic matter, including residual oil and phenolic compounds. The distinctive physicochemical properties of WOMP require specific management solutions and have prompted the adaptation of conventional valorization strategies for olive mill pomace.

Composting is among the suggested alternatives for the valorization of WOMP, and it is particularly compelling because of the low organic matter content in agricultural soils within the Mediterranean region (Ferreira et al., 2022). Thus, composting WOMP bridges the gap between waste reduction and soil enrichment, benefiting both farmers and the environment. However, most of the physical and chemical properties of WOMP, including very low porosity, high moisture, low contents of N and P, or antimicrobial activity (attributable to polyphenols), are not well-suited for composting. Nonetheless, the effectiveness of co-composting WOMP with complementary wastes generated in the vicinity, such as olive tree pruning residues and animal manures (a source of N and P) has been demonstrated (Canet et al., 2008). Currently, composting facilities are being established in olive oil-producing areas but there is still a need for reliable and efficient indicators of compost maturity to maximize the benefits of compost application in sustainable agriculture. The degree of organic matter stabilization in compost during the mineralization and humification processes is referred to as compost maturity. Several indices (e.g. C/N, C/H, O/H, E₄/E₆, etc.) are usually combined to assess the maturity of compost (Droussi et al., 2009; Fialho et al., 2010). However, these methods often require chemical or biological analyses in the laboratory, which are also typically time- and money-consuming.

Recent studies have highlighted the potential of spectroscopic methods for evaluating compost maturity (Martín et al., 2023). In particular, three-dimensional excitation-emission matrix (EEM) fluorescence spectroscopy has been revealed very useful for the characterization of organic matter (OM) in compost water extracts (WEs) (Wang et al., 2023; Wei et al., 2016; Zhao et al., 2017). These studies have reported that the fluorescence characteristics of OM in compost reflect the gradual decomposition of protein-like substances during composting, as well as the formation of fulvic- and humic-like substances. However, the photophysics of the dissolved OM is very complex (Wells et al., 2022), even when only a fraction of the organic matter molecules contains light-absorbing functional groups in the UV-Vis region. The interpretation of the changes in position and intensity of EEM peaks observed in WEs from compost has typically relied on previous studies on dissolved organic matter (DOM) from freshwater, coastal waters, and wastewaters (Murphy et al., 2008; Wünsch et al., 2017; Yang et al., 2015). However, differences in both excitation and emission wavelengths are observed. The proposal to use PARAFAC analysis to decompose the fluorescence EEMs of water-extracted OM from a wide range of compost samples at different maturity stages was first introduced by Yu et al. (2010). Fulvic-like and protein components were found more suitable to assess compost maturity than humic substances. Furthermore, Wei et al. (2014) reported discrepancies between the fluorescence regional integration of EEM and traditional fluorescence spectra. This study suggested that fulvic acids may be the main component in WEs of compost, while the observed humic acid regions in conventional fluorescence spectra could potentially represent highly aromatized fulvic acid. In fact, the complexity associated with the interpretation of an EEM is often overlooked (Rosario-Ortiz and Korak, 2017).

Considering all the previous studies, it is clear that further research is still necessary to gain a comprehensive understanding of the fluorescent behavior of compost WEs particularly in relation to the association of EEM regions with operationally defined OM fractions. Furthermore, the analysis of chemical properties during two-phase olive mill pomace composting reported in previous studies has shown the peculiar nature of this substrate (Cayuela et al., 2008). Given the limited information available on the fluorescence features of this type of compost, it deserves a more in-depth study. Thus, the goals of this work are: (i) to provide further insight into the transformations of OM during WOMP co-composting by studying the fluorescence characteristics of compost at different stages of the process in a composting facility at an industrial scale; (ii) to compare the fluorescence features of WEs from compost with those of the different fractions derived from the operational definition of humic substances (HS) (based on their solubility at low pH, and adsorption to XAD resins); and (iii) to study the relationship between several parameters of agronomic interest and the PARAFAC components from WEs as an alternative for effective compost maturity assessment.

2. Material and methods

2.1. Composting plant operation and sampling strategy

Samples were obtained from INGNIA S.L., a composting plant located in Almedinilla (Córdoba, Andalucía, Spain). As input material, the plant employed a mixture of 68% wet olive mill pomace (WOMP) from olive mills of the region; 20% goat manure mixed with straw (GM); 9% olive tree pruning (OTP), and 3% chicken manure mixed with sawdust. OTP, straw and sawdust were added as bulking agents to ensure efficient decomposition. Windrow composting was performed in an open pile (80 m (L) x 6 m (W) x 4 m (H)). The formation of the pile started at the beginning of the olive harvesting season and lasted throughout the oil production campaign (from November 2020 until March 2021). After the pile was completed, aeration was maintained by turning it once a month until November 2021. As a sampling strategy, the pile was arbitrarily divided into 4 sectors of 20 m in length (S1 to S4; Fig. S1). In this way, the progressive growing in length of the pile by addition of fresh material was considered. Each sample involved five sub-samples collected in different pile positions (height and depth) of the corresponding sector (see Fig. S1). Therefore, 47 compost samples were collected during the whole composting process. All the samples were desiccated at 65 °C, then ground and sieved to 200 µm.

2.2. Physical-chemical characterization

Moisture content was determined gravimetrically by drying the samples at 105 °C for 24 h and measuring the weight loss. Electrical conductivity at 25 °C (EC₂₅) and pH were determined in 1:10 (w/v) water extracts using an EC-meter CRISON Basic 30 (HACH LANGE, Spain) and a HI5221 pH meter (HANNA® Instruments, Australia), respectively. Determination of carbon, hydrogen, and nitrogen was conducted in a TruSpec CHN 620–100–400 (LECO Corporation, USA) elemental analyzer. The organic matter (OM) and ash content of the compost were determined using the "loss-on-ignition" (LOI) method, which entailed combustion in a muffle furnace at 550 °C for 5 h (Nelson and Sommers, 1982).

The cation exchange capacity (CEC) was determined using the spectrophotometric method proposed by Aran et al. (2008), based on the decrease of absorbance of a hexaamminecobalt(III) chloride, [Co(NH₃)₆]Cl₃, solution. Briefly, 0.5 g dry COMP was placed in 50 ml polypropylene tubes with 20 ml of 0.05 N [Co(NH₃)₆]Cl₃ solution. After continuous shaking for one hour (110 rpm), solutions were decanted and filtered (0.22 µm). Absorbance values of the resulting solutions and 0.05 N [Co(NH₃)₆]Cl₃ solution were immediately measured at 472 nm.

Total phenolic content (TPC) was assessed using the Folin-Ciocalteu colorimetric method (Pontoni et al., 2017). The extracts were obtained in triplicate by stirring 0.25 g of dried and sieved compost with 5 ml of pure methanol for 30 min. Subsequently, the mixture was centrifuged at 3000 rpm for 10 min, and the resulting supernatants were stored at 4 °C until analysis. To 250 µl of extract, 1.25 ml of the Folin-Ciocalteu reagent and 1 ml of 7.5% Na₂CO₃ were added. The solution was then diluted to 5 ml with Milli-Q® water (obtained with a Millipore Milli-Q® Integral 5 water purification system, Serv-A-Pure USA). After a dark incubation period of 30 min and subsequent color development, the absorbance was measured at 765 nm in a ZUZI spectrophotometer model 4201/50 (Auxilab, Spain). The TPC of the samples was calculated using a calibration curve established with gallic acid standard solutions and expressed as milligrams of gallic acid equivalent per gram of dry weight (mg GAE g⁻¹ DW).

2.3. Organic matter extraction

To prepare water extracts (WEs), 4 g of dry samples were moistened with ultrapure Milli-Q® water to 60% water holding capacity and let stand for 30 min. Then, Milli-Q® water was added to a 1:10 (w/v) concentration and stirred mechanically for 30 min, centrifuged at 3000 rpm for 15 min, and filtered (0.45 µm).

Furthermore, selected samples underwent alkaline extraction and organic matter fractionation following a procedure adapted from previous studies (Swift, 2018; Yu et al., 2018). Samples (0.5 g) were extracted with 30 ml of 0.1 M NaOH + Na₄P₂O₇ under N₂, and shaken for 24 h at 60 °C. After centrifuging at 2500 rpm, 20 min, and filtering through 0.45 µm, the supernatant was obtained, containing the total alkali-extractable organic-C fraction (including HA and AS). To precipitate humic-like substances (HA), the filtrate was acidified to pH ≤ 2 using H₂SO₄ 96%, and allowed to stand for 1 h. The resulting acidified solution (AS) was then separated from the HA by centrifugation (3000 rpm for 10 min).

The precipitate (HA) was re-dissolved with NaOH 0.5 M and again acidified with H₂SO₄ 96%, for an additional clean-up. After standing for 6 h and centrifugation (2500 rpm, 15 min), HA purification was performed by water washing, dialysis (with a dialysis membrane of 12–14,000 Daltons), and lyophilization. The HA fraction was redissolved in alkali for spectra recording.

The supernatant (AS) was separated into fulvic-like acid (FA) and non-humified organic matter (NH-OM) fractions by adsorption through a cleaned poly(vinylpyrrolidone) resin (PVP, ~110 µm particle size). The FA were retained and then eluted by resin backwashing with NaOH 0.5 M.

2.4. Agronomic characterization

The Zucconi test was used to estimate the germination index (GI) as a basic agronomic assay (Zucconi et al., 1981). 1 ml of the WE was added to a Petri dish containing filter paper and 10 *Lepidium sativum* L. seeds were then incubated at 28 °C for 72 h in the dark. Then the number of seeds germinated was counted and the root length of those germinated was measured. The results were expressed as the GI, which represents the percentage of germination and root elongation compared to the control sample (incubated with Milli-Q® water). Germination indices below 60% indicate high toxicity; those between 60% and 100% represent acceptable or normal stages; while values exceeding 100% signify high-quality samples that favor root growth.

2.5. Fluorescence spectroscopic characterization

The WEs of all compost samples and the selected isolated fractions of alkaline extracted OM were studied by fluorescence spectroscopy. Furthermore, spectra of commercial standards of several fluorescent substances reported to occur in WOMP were registered for comparison: gallic acid monohydrate (> 98%, A.C.S. reagent, Sigma Aldrich, USA); humic acid (Sigma Aldrich, USA); alkali lignin (Sigma Aldrich, USA); guaiacol (Sigma Aldrich, USA); 2,6-dimethoxyphenol (99%, Sigma Aldrich, USA); tannic acid (A.C.S. reagent, Sigma Aldrich, USA); and verbascoside (HWI group, Germany).

Fluorescence spectra were recorded with a Cary Eclipse fluorescence spectrometer (Varian Inc., Mulgrave, Australia) in a clear quartz cuvette (1 cm). Cary-Eclipse (Varian Inc.) software package was employed for data collection. The slit widths for both excitation and emission monochromators were set at 5 nm, and the scan speed was 120 nm min⁻¹. Emission spectra in the range of 370–600 nm were detected at an excitation wavelength of 348 nm. Excitation spectra were obtained over a range of 260–400 nm, establishing an emission wavelength of 430 nm. Synchronous-scan excitation spectra were obtained between 240 and 600 nm with a constant offset of

$\Delta\lambda = 30 \text{ nm}$ (He et al., 2011).

Fluorescence excitation-emission matrices (EEMs) spectra were measured as follows. Emission (Em) wavelength was scanned from 240 to 600 nm at 2 nm increments varying the excitation (Ex) wavelength from 220 to 400 nm at 5 nm increments. The scan rate was 1200 nm min^{-1} , and the voltage of the photomultiplier tube (PMT) was set at 650 V for low-level light detection. Each data matrix was composed of 177 Em (rows) \times 37 Ex (columns) wavelengths.

2.6. Statistical analysis

Pearson's correlation coefficients were calculated using Statgraphics Centurion XIX software (Statgraphics Technologies, Inc., USA). The correlations were considered statistically significant at a 95% confidence interval ($p \leq 0.05$).

All the chemometric treatments were performed using Solo+MIA software version 8.9.1 (Eigenvector Research, Inc., USA). Principal component analysis (PCA) was used to explore patterns among samples and variables. In this sense, PCA scores were used to correlate the most relevant spectral features described by the principal components (PCs) and the compost samples. Emission and excitation fluorescence spectra were together analyzed by merging their information. Thus, a low-level data fusion strategy was applied by concatenating the spectra. Preprocessing steps before PCA model development comprised smoothing, baseline correction, mean-centering, and normalization. The same preprocessing was used for the synchronous spectra.

To analyze the fluorescence EEMs' multivariate data, parallel factor analysis (PARAFAC) was used. First, subtraction of EEM spectra of Milli-Q® water, as well as first and second-order Rayleigh scattering removal (15 and 20 nm filters, respectively), were performed.

The PARAFAC is a powerful chemometric tool for multi-way data analysis of EEM spectra, based on the assumption of a linear relationship between Ex-Em wavelength pairs. Its primary application is to determine the number of components responsible for the features observed in each spectral signature. As fluorescence EEMs are arranged in a three-dimensional data matrix ($X = I \times J \times K$), the PARAFAC algorithm decomposes it into a sum of the triple product of vectors (components or factors) and a matrix of error e (Eq. 1). In PARAFAC for each component (or factor), there is one score (A) and two loadings (B-C) vectors, which are organized into spectral matrices (a-c). Each matrix represents a different dimension of the original data cube consisting of N factors (with N being the minimum number of independent factors needed to effectively depict the data variances) (Yu et al., 2010).

$$X_{ijk} = \sum_{n=1}^N a_{in} b_{jn} c_{kn} + e_{ijk} \quad (1)$$

where ijk is the fluorescence intensity of sample k at excitation wavelength i and emission wavelength j .

Here, each fluorophore in the system will result in a PARAFAC component. The scores of these components can be assigned to represent the corresponding relative concentrations. The appropriate number of components was determined by studying both the core consistency (Bro and Kiers, 2003) and the percentage of explained variance. A core consistency of 100% indicates a fully trilinear model. For this study, a nonnegative constraint was enforced to allow only chemically feasible and pertinent results.

3. Results and discussion

3.1. Preliminary physical-chemical characterization of compost samples

Typical parameters for the physical-chemical characterization of the compost samples were determined. The results for the first and last compost samples collected from each sector of the pile are summarized in Table S1. In general, samples collected in the early stages of composting (≤ 8 weeks) were characterized by high moisture contents (60–50%) and low pH (below 7), resembling those typical of raw WOMP (Roig et al., 2006). Nevertheless, initial samples from sampling sectors S3 and S4 showed lower values of humidity, probably due to climatological issues during pile formation. The high initial EC₂₅ values may be associated with the incorporation of animal manure into the composting mixture, added to increase the N content, mainly in the form of urea (Nahm, 2003). As composting proceeds, a progressive decrease in moisture content can be observed, along with increasing pH values.

Variations in the initial values of the C/N parameter (25–30) highlight the heterogeneity of the raw materials used in the composting process. The C/N ratio consistently decreased during the initial weeks of composting, typically reaching values below 20 at the end of the process. This follows the current Spanish regulation (BOE, 2017), which establishes a maximum C/N ratio of 20 for composted olive mill pomace. In addition, a decrease in H content and LOI with composting due to the degradation of organic matter was also observed. On the contrary, the CEC of compost, which can be used as an index to evaluate nutrient retention ability, increased with maturation due to the incorporation of carboxyl and phenolic groups in humified materials.

TPC is a parameter with a specific regulation (BOE, 2017) for WOMP compost since polyphenols are demonstrated to be phytotoxic (Pinho et al., 2017). A wide range of phenolic compounds have been reported in WOMP, including simple phenolic alcohols and acids, phenolic glucosides, phenolic oleosides, and flavonoids (Artajo et al., 2007) as a consequence of the partition of phenolic compounds between the oil and the byproducts during olive oil extraction (Ait Baddi et al., 2009). Thus, the phenolic content in this material is relatively high, causing strong phytotoxic and antimicrobial effects. It is interesting to note that sector 4, built until May'21, showed the lowest initial value of TPC. This can reflect the characteristics of the raw material, WOMP, produced at the end of the harvest season with overripe olives. In any case, a significant reduction of the TPC content (around 70%) during the composting process was observed. In fact, polyphenols are considered to act as the carbon skeleton of polymerization or polycondensation reactions leading to

humification, being the polyphenol humification pathway essential for compost maturation processes (Xu et al., 2022).

Finally, the germination index is widely used as an indicator of compost phytotoxicity and hence maturity (Tian et al., 2012). According to our results, the severe phytotoxicity of fresh compost WEs (GI < 20% in all cases), probably due to both the high polyphenol content and the presence of residual fatty acids, was significantly reduced by composting. Thus, GI increased up to about 60% for mature compost, which can be considered phytotoxicity-free (Zucconi et al., 1981). These GI indexes are not optimal and could be due to the relatively elevated values of EC₂₅. Nevertheless, these values are similar to those reported in previous studies for compost obtained from different olive mill residues, with GI values typically ranging from 45% to 88% (Michailides et al., 2011).

3.2. Conventional fluorescence spectroscopy measurements

Due to the scarcity of information on the fluorescence characteristics of WOMP compost, we initially recorded the excitation, emission, and synchronous fluorescence spectra of WEs of this material at different stages of maturation. The excitation spectra of the compost WEs showed a complex pattern due to the superposition of several bands between 275 and 375 nm, as shown in Fig. S2. The area under the entire curve of the excitation spectra (A_{EX}) was calculated, revealing a positive correlation with composting time ($R = 0.572$; $p < 0.001$). Furthermore, the emission spectra exhibited a broad band between 400 and 500 nm (Fig. S2b). The area of the emission spectra (A_{EM}) also correlated with composting time ($R = 0.721$; $p < 0.001$).

The synchronous-scan fluorescence spectra are particularly interesting as they reflect the combined spectra of diverse fluorophores contained in the organic matter and are better resolved than the excitation and emission spectra. In order to describe the spectral features and to relate them with the composting time, four regions were considered and the corresponding areas were calculated (A_A , A_B , A_C and A_D) (see Fig. 1 and Table 1).

The region between 240 and 300 nm (A), can be linked to proteinaceous materials and other monoaromatic compounds (Santos et al., 2010), including simple polyphenols. The area, A_A , showed a negative correlation (see Table 1) with composting time for the four sectors considered during sampling in the pile.

The bands in the region B (300–410 nm), indicate the presence of polycyclic aromatics consisting of 3–4 fused benzene rings and 2–3 conjugated systems in unsaturated aliphatic structures (Santos et al., 2010). This region is also associated with more complex compounds like guaiacol and tannic acid, by comparison with the fluorescence spectra of commercial standards.

Region C (410–480 nm) is attributed to polycyclic aromatics with about 5–7 fused benzene rings (He et al., 2011). The area of these two regions, A_B and A_C , showed a positive correlation with the number of composting weeks. These findings reflect an increase in the molecular size of the fluorophores with composting in agreement with other studies in different types of compost (He et al., 2011; Richard et al., 2009).

Finally, region D is characterized by a band centered at 500 nm, especially intense in samples collected at earlier stages in sampling sectors 1 and 2. This is evident in the strong negative correlation between time and A_D for these two sectors. For S4, the correlation with A_D , although still negative, is much lower, implying a lower contribution of the responsible compounds. This band at 500 nm, which has not been described in previous studies on compost, was also detected in the OM of fresh olive mill pomace (see Fig. S3). This observation may be associated with the oxidized and polymerized forms of complex polyphenols. Additionally, pectin, present in high amounts in WOMP could contribute to the shift of the fluorescence emission band towards longer wavelengths by forming cross-links with the aromatic rings of polyphenols (Hu et al., 2023). The degradation of polyphenols and pectin in overripe olives (González-Cabrera et al., 2018; Mafra et al., 2001) can explain the lower contribution of this band in samples of S4 since this part of the composting pile was formed with WOMP produced at the end of the harvest season.

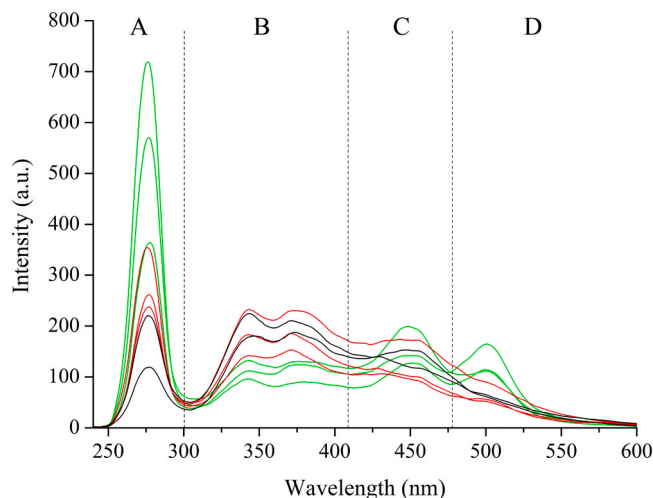


Fig. 1. Synchronous-scan spectra of WE at different stages of the composting process: ■ initial stage (Dec. 2020, Jan. 2021 and Feb. 2021); ■ middle stage (May 2021; July 2021 and Aug. 2021); ■ final stage (Sep. 2021 and Nov. 2021).

Table 1

Pearson's correlation coefficients for composting time (weeks) and the areas in the different regions (A_A , A_B , A_C , and A_D) for each sampling sector of the pile.

Sector	A_A (240–300 nm)	A_B (300–410 nm)	A_C (410–480 nm)	A_D (480–600 nm)
S1	-0.572*	0.858*	0.862*	-0.855**
S2	-0.755**	0.995***	0.728**	-0.705**
S3	-0.668*	0.784**	0.814**	-0.610*
S4	-0.549*	0.551*	0.584*	-0.228*

Statistical significance: * $p < 0.05$; ** $p < 0.01$; *** $p < 0.001$.

For a better understanding of the most relevant fluorescence spectral features that occurred during composting, PCA was performed. A low-level data fusion strategy was employed by merging the conventional fluorescence spectra of each sample. This approach ensured that both excitation and emission spectral features were considered in obtaining the loading vectors. The results of PCA are presented in Fig. 2.

As can be seen in the PCA score plot (Fig. 2a), there is a shift in the distribution of the samples towards more positive values of PC1 (48.31% variance explained) as the composting progresses. Thus, samples collected between Dec. 2020 and Feb. 2021 (mostly from S1 and S2) showed negative PC1 values, whereas those samples collected from Aug. to Nov. 2021 (across all sampling sectors) tend to show more positive values. The inspection of the loadings plots (Fig. 2b) provides insights into the changes occurring in both the emission and excitation spectra during composting. As composting advances, the fluorescence intensity at 270 nm excitation decreases, while it increases with excitation at around 314 nm showing two defined shoulders at 326 and 337 nm. Excitation in this zone may be associated with aromatic compounds of fulvic acid-like nature, in line with findings reported by Huo et al. (2008). Regarding the emission wavelength, it is observed that more mature compost samples are characterized by higher fluorescence intensities

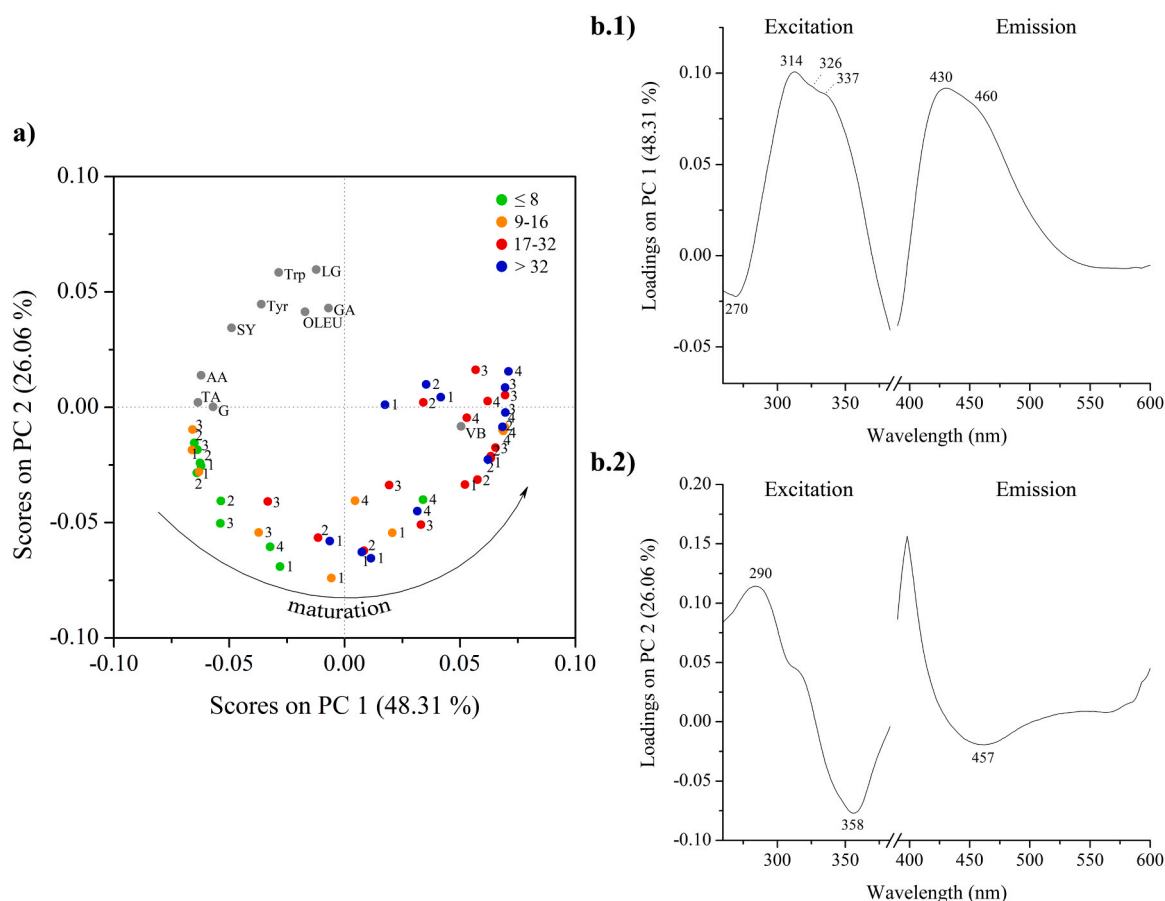


Fig. 2. PCA results for the analysis of data fused emission and excitation spectra of WEs and standards. a) Scores plot. Samples are labeled according to composting weeks (by color, legend information in the plot) and sampling sectors (1–4); Acronyms for commercial standards: AA: amino acids; G: guaiacol; GA: gallic acid; LG: lignin; OLEU: oleuropein; SY: syringol; TA: tannic acid; Trp: tryptophan; Tyr: tyrosine; VB: verbascoside. b) PC1 (b.1) and PC2 (b.2) loading vectors.

between 430 and 460 nm. This observation can be indicative of a higher degree of polymerization of the organic matter (Milori et al., 2006). In addition, the samples collected during the initial stages of composting are grouped in PC1 together along with the majority of the measured commercial standards. PC2 (accounting for 26.06% of the variance) contributes mainly to differentiating the standards (generally simpler structures) from the compost extracts. This differentiation is reflected in the PC2 loadings, with excitation at 290 nm for the former and at 358 nm for the latter. Furthermore, compost extracts are characterized by the broad emission band centered at 457 nm, which is typical of complex humified organic matter. Only verbascoside, a phenylethanoid glycoside that is more complex and has a higher molecular mass than monomeric phenols, clusters with the more mature compost samples (for both PC1 and PC2). Therefore, the results indicated that the decay of proteins, lignin, and monomeric phenols are the primary precursors in the formation of stabilized humic-like organic matter (Said-Pullicino et al., 2007). In the analysis of synchronous spectra, the PCA did not reveal such clear trends with composting time, possibly due to the complexity introduced by the already commented band at 500 nm present in the fresh material.

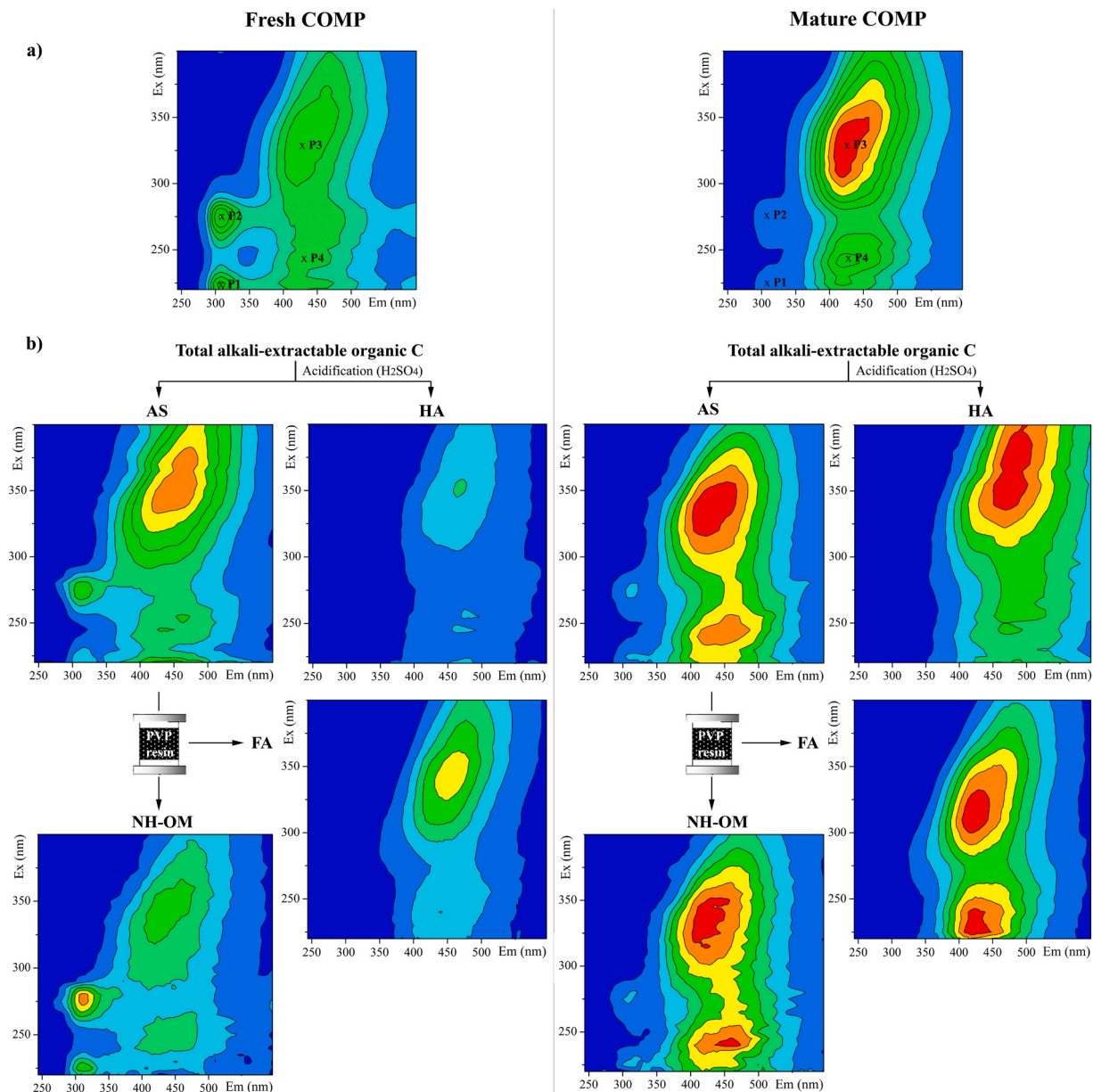


Fig. 3. Typical EEM spectra of a) compost water extracts and b) the different organic matter isolated fractions derived from alkaline extraction obtained, from fresh (≤ 8 weeks, left) and mature (> 32 weeks, right) compost. AS: acidified solution; HA: humic-like substances; FA: fulvic-like substances; NH-OM: non-humified organic matter; PVP: poly(vinylpyrrolidone) resin.

3.3. EEM Fluorescence Spectroscopy with PARAFAC analysis

Fluorescence excitation-emission matrices (EEM) of compost WE at different maturation stages as well as OM fractions derived from the operational definition of humic substances were obtained and compared (see Fig. 3). The study of the fluorescence features of the different fractions can provide further insight into their chemical nature along the process of composting. As can be seen in Fig. 3a, the typical EEM spectra of WE non-evolved samples are featured by two main peaks at Ex/Em of 220/318 nm (P1), and 275/332 nm (P2). As composting proceeds, these two peaks tend to diminish in intensity and even disappear. Furthermore, a peak centered at 330/420 nm (P3) is also observed in both non-evolved and evolved compost being much more intense in the latter where a new peak at 245/430 nm (P4) also emerges.

The EEM contours for the OM fractions isolated according to the conventional procedures (Swift, 2018; Yu et al., 2018) are shown in Fig. 3b together with a scheme of the fractioning procedure. As can be seen, the EEM spectra of the substances remaining in the solution after acidification (AS) strongly resemble those of compost WEs, for both non-evolved and evolved samples showing the already described P1 to P4 peaks. The HA fraction, extracted by alkali and re-precipitated by acidification, shows much more intensity for P3 for the evolved samples. The position of the band is slightly shifted to higher Ex/Em wavelengths in comparison with the band observed in WEs. After purification of AS, the FA fraction obtained in non-evolved samples is free from P1 and P2 contributions, which clearly correspond to non-humified organic matter. In the case of evolved samples, the intensity of P3 and P4 is enhanced in the FA fraction although these contributions also appear in the fraction of non-retained substances.

The strong fluorescence overlap in 3D fluorescence data makes difficult the direct interpretation of EEM representations and may lead to wrong assignments. Thus, Parallel Factor Analysis (PARAFAC) was used to extract the components and to identify the main fluorophores contributing to the compost maturation process. Pre-processing of the fluorescence EEMs was performed to remove Rayleigh and Raman scattering prior to determining the number of components. A sudden drop in core consistency was observed from a 3-component model, which had a consistency of 99%, to a 4-component model with 45%. This, along with the 86.23% explained variance, indicated that a 3-component model was appropriate for the current data set. It is worth noting that the PARAFAC analysis was applied to different randomly built data sets to assess its stability. This demonstrated the consistency of the PARAFAC analysis with no sample dataset size requirement.

Fig. 4 shows the pure emission and excitation spectra of the three components obtained by PARAFAC decomposition of the EEM spectra. A comparison of the Ex/Em wavelength pairs calculated for each component in WOMP with previous studies (Guo et al., 2012; Liu et al., 2009; Murphy et al., 2008; Yuan et al., 2018) can be found in Table S2. C1 and C2 were assigned to fulvic-like (or microbial fulvic-like) and terrestrial humic-like components, respectively. As can be seen in Fig. 4, C1 and C2 exhibited a unique emission maximum with different excitation wavelengths. This is attributable to the rapid internal conversion of the excited electrons to the lowest vibrational level of the first excited state (Lu et al., 2009). The ΔEx between primary and secondary peaks is greater for C2 (110 nm) than for C1 (80 nm), in agreement with the typical behavior described for humic and fulvic acids (Wells et al., 2022). Previous studies using high-resolution mass spectrometry (FT-ICR-MS) found that fluorescent components with characteristics similar to C2 (with long excitation and emission wavelengths) involve oxygen-rich, aromatic structures with high apparent molecular weight (Kellerman et al., 2015). In contrast with earlier views of humic acids, these substances do not represent large macromolecules with physically defined MW and diverse functional moieties, but supramolecular aggregates of relatively high MW ($\sim < 1000$ Da) diverse molecules associated via hydrophobic interactions and hydrogen bonds (Stubbins et al., 2014).

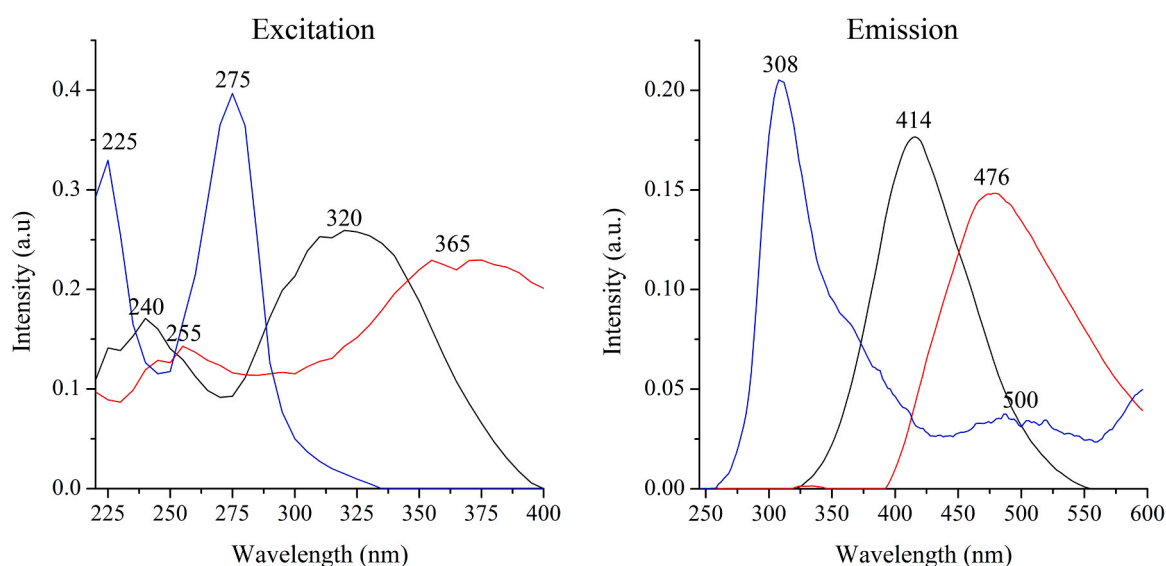


Fig. 4. Excitation and emission mode loading vectors from three components PARAFAC model of fluorescence data of compost samples. Colors refer to PARAFAC components: C1 (black); C2 (red) and C3 (blue).

Interestingly, the protein-like component C3, in addition to the fluorescence typical of tyrosine ($\text{Em } 308 \text{ nm}$) and tryptophan (reflected in the loading as a shoulder at 344 nm), shows another emission maximum at 500 nm . This emission band, although overlaps with the fluorescent emission of C2, resembles the one observed in the synchronous spectra of WOMP (Section 3.2). PARAFAC emission loadings with multiple peaks have been depicted previously, but they have long remained unexplained or ignored. Recently, Wells et al. (2022) attributed these components exhibiting two fluorescence maxima (one located in the protein region and the second one in the fulvic or humic regions) to interactions between protein-like and diagenetic-like (humic) compounds in dissolved organic matter. Supramolecular interactions must be responsible for the two emission maxima observed in this study as well. Here, the interaction probably involves protein and polyphenols together with pectin, as previously discussed for the band at 500 nm observed in the fresh WOMP synchronous spectrum (Fig. S3).

The PARAFAC model was first used to compare the composition of the different OM fractions isolated from alkaline extracts of compost and WEs, according to the score vectors of each component. The relative concentrations of each component are shown in Fig. 5 for two compost samples (from S3) at different maturity stages. Similar results were obtained for the rest of the sampling sectors (data not shown).

The relative abundance of the three components in the WEs is obviously lower than in all the fractions obtained by the more effective alkaline extraction. Furthermore, as can be seen in Fig. 5, the three PARAFAC components are present in all the isolated fractions. It is clear that FA and HA are operational definitions that do not represent distinct chemical subgroups, and therefore cannot be directly associated with distinct PARAFAC components calculated on the basis of differences in the fluorescence features. Additionally, the fractioning methodology makes it impossible to distinguish whether the extracted organic matter truly corresponds to a humic-like material or non-humic organic matter with similar solubility properties. This distinction can be particularly relevant in the early stages of the composting process, dealing with poorly humified fresh material. Despite all these challenges, interesting information about the changes in composting can be inferred from this study. The behavior of components C1 and C3 with composting time is very similar in WEs and alkaline extracted fractions, particularly in AS fractions. A decrease in C3 (associated with simple aromatics like proteins, and other soluble microbial by-product materials (SMP)) and an increase in fulvic-like compounds (C1) is observed as composting proceeds. During the earliest composting stages, the larger molecules break down into smaller and more soluble ones, leading to the temporarily greater availability of substrates for the microorganisms, thus increasing their metabolism. As the process advances, there is a drop in the level of microbial activity, and proteinaceous compounds and polyphenols are incorporated into fulvic acid-like frameworks in the bio-oxidation phase of composting (Plaza et al., 2007; Zhang et al., 2016). However, the main change with maturity occurs in the HA fraction where an important rise in C2 (associated with high molecular weight aromatic humic-like substances) was observed. Interestingly, this trend was not found in the corresponding WEs, which do not show a strong increase in C2 with maturity. This finding is in agreement with the results reported for EEM of WEs in other types of compost. Thus, components similar to C1 and C3 were found to be more suitable for assessing compost maturity than C2 (Yu et al., 2010). Additionally, other authors (Huang et al., 2019) observed a reduction in the proportion of humic-like to fulvic-like components, suggesting that the latter were preferentially generated during composting. Our results demonstrate that humic-like substances are produced indeed during compost maturation. However, the lower solubility of these humic-like substances in water in comparison with fulvic-like ones is responsible for their less effective extraction and therefore explains the inconsistency of the results observed in previous studies. Thus, the amount of HA substances formed during composting has been probably underestimated in previous studies that were focused only on the study of compost WEs. The presence of these humic-like materials in compost holds significant importance as they mimic the behavior of natural soil organic matter. Consequently, they can profoundly influence various soil properties and functions, including the reduction of soil bulk density, enhancement of soil structure and stability, as well as the mitigation of water runoff and soil erosion (Ferreira et al., 2022).

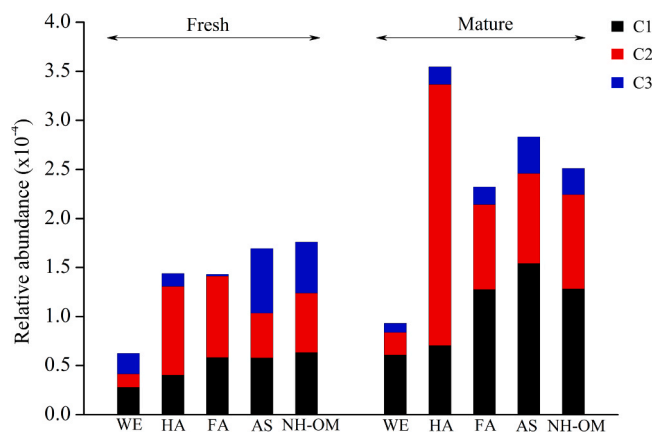


Fig. 5. Contributions of the PARAFAC components in fresh (F; ≤ 8 weeks) and mature (M; > 32 weeks) compost samples. WE: water extract; HA: humic fraction and FA: fulvic fraction. AS: acidified solution and NH-OM: non-humified organic matter, according to the scheme in Fig. 3.

3.4. Relationships between OM fluorescent components and compost maturity parameters

Correlations between maturity parameters (refer to Section 3.1) and the scores of PARAFAC-derived components were first investigated to provide further insight into OM transformations during composting and to assess the capability of EEMs for maturity assessment. WEs were selected for this study because their faster preparation procedure compared to the isolation of HS fractions. Furthermore, WEs represent better the short-term behavior of compost after application on soils. Results are summarized in Table 2.

As expected from the previous results interpretation, C1 and C2 were strongly correlated ($R = 0.80$; $p < 0.001$). Both C1 and C2 were positively correlated with composting time (W), although the correlation was less significant for C2, due to the already discussed lower solubility of humic-like compounds. The C/N ratio is one of the most important indices used for the evaluation of the composting process and compost maturity. In this regard, the scores of the 3 components showed significant correlations with it ($p < 0.01$), these being negative in the case of C1 and C2 ($R = -0.39$ and -0.43 , respectively) since the C/N ratio decreases as organic matter degrades and material stability increases; while it correlated positively with C3 ($R = 0.70$; $p < 0.001$). The strong negative correlation observed with H content for C1 and C2 reflects the loss of aliphatic moieties and the increase in aromaticity in these fluorophores in comparison with C3 (which showed a positive correlation). Humification is related to increments in the aromatic character of the molecules, which may be reflected in the presence of more condensed polyaromatic structures as well as to the possible increase in the conjugation degree in unsaturated aliphatic chains. Furthermore, the highest correlation was found between CEC and both C1 and C2. This reflects the accumulation of acidic functional groups, mainly phenolic and carboxylic acids, in humified materials. On the other hand, the strong positive correlation between TPC and C3 ($R = 0.75$; $p < 0.001$), supports the proposed hypothesis of an interaction between proteinaceous materials and polyphenol-related compounds during the initial stages of WOMP composting. This fact would also explain the negative correlation of C3 with GI ($R = -0.58$; $p < 0.001$) since polyphenols can be phytotoxic.

To further investigate the relationships between the different parameters, PCA modeling was performed. The results are presented in Fig. 6.

As can be seen, there is a certain trend of differentiation of the compost samples according to their composting time along the PC1 axis (47.49% explained variance). Thus, more mature samples (in the negative PC1 region) present a higher contribution of humic and fulvic-like components (C1 and C2), and fresh compost samples have higher content in C3 (mostly protein-like components). The information contained in the PCA model developed confirms our previous findings regarding the relationships between PARAFAC components and conventional maturity parameters. In particular, C2 and CEC are very close in the space defined by PC1 and PC2, which highlights the important function of HA as ion-exchange systems. This study also provides some insight into differences in the composting process depending on the sector of the pile. Thus, considering also the PC2 axis (16.96% explained variance), the increase in C1 and C2 seems to take longer in sampling sector S1 (see the group of S1 samples, with the composting time of 9–16 weeks, and strong negative values for PC2). This could be associated with less efficient biodegradation of OM in this sector of the pile due to multiple reasons, including cold weather and insufficient oxygenation. Furthermore, the higher resistance to biodegradation of WOMP from olives harvested at early stages of ripeness in comparison with those processed at the end of the season (S3 and S4) can also have an impact. These data help in understanding the difficulties in producing a standardized WOMP compost in the long-term at a full-scale facility under usual working conditions and also highlight the need of using representative sampling methods, considering the heterogeneity that occurs in large composting piles. As seen in Fig. 6, considering both PC1 and PC2, mature compost samples suitable to be used as organic amendments, are characterized by optimal C/N ratios ($C/N < 20$, according to the Spanish R.D. 999/2017 on fertilizer products (BOE, 2017)), and a more humified and stable organic matter, with higher CEC. They also present a lower percentage of phytotoxic compounds such as polyphenols, as well as higher EC_{25} and pH values, together with beneficial effects on seed growth ($> GI$).

4. Practical applications and future research prospects

The obtained results clearly illustrate how PARAFAC-derived components are useful for elucidating organic transformation during composting, and how they can also be related to parameters of agronomic interest to assess maturity. Considering the singular fluorescence features of component C3 and the differences observed in the behavior of the different sampling sectors of the composting pile, more research should be conducted to elucidate the influence of different factors in the composting process, in particular, the ripeness stage of the olives.

On the other hand, the comparison of EEMs of compost WEs and classical OM fractions has revealed interesting aspects that require

Table 2

Pearson's correlation matrix for compost maturity parameters and the scores of PARAFAC-derived components.

	C2	C3	W	pH	EC_{25}	C/N	H	LOI	CEC	TPC	GI
C1	0.80***	-0.18*	0.50***	-0.07	0.29**	-0.39**	-0.60***	-0.29*	0.54***	-0.39**	0.19
C2		-0.57**	0.36**	0.24	0.17	-0.43**	-0.55***	-0.32*	0.56***	-0.35**	0.28
C3			-0.35*	-0.69***	0.11	0.70***	0.49***	0.28	-0.27	0.75***	-0.58***

C1, component 1; C2, component 2; C3, component 3; W, composting weeks; EC_{25} , electrical conductivity (25 °C); C/N: carbon to nitrogen ratio; H, total hydrogen (%); LOI, organic matter calculated as "loss-on-ignition"; CEC, cation exchange capacity; TPC, total phenolic content; GI, germination index.

Statistical significance: * $p < 0.05$; ** $p < 0.01$; *** $p < 0.001$.

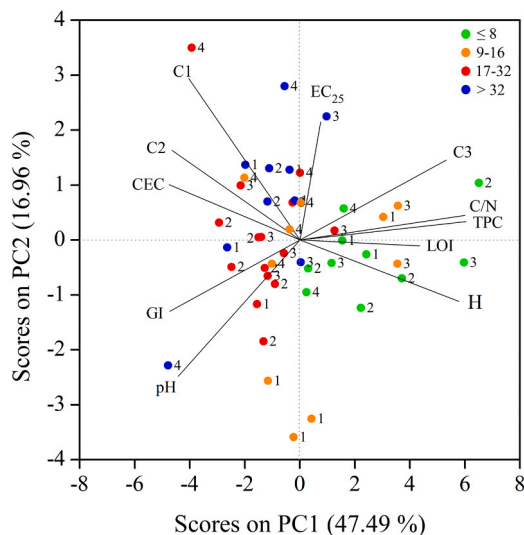


Fig. 6. PCA score-loadings biplot of the maturity parameters (EC₂₅: electrical conductivity (25 °C); H: total hydrogen (%); C/N: carbon to nitrogen ratio; LOI: organic matter expressed as “loss-on-ignition”; CEC: cation exchange capacity; TPC: total phenolic content; GI: germination index) and PARAFAC-derived components (C1, C2 and C3) of the compost samples. Samples are labeled according to composting weeks (by color, information in the plot) and sampling sectors (1–4).

further investigation as well. Mature WOMP compost are demonstrated to be richer in humic-like substances than suggested by results based only on WEs. Thus, solid phase fluorescence could be an interesting complementary approach allowing rapid analysis of samples without any prior chemical treatment.

5. Conclusions

A comprehensive characterization of the fluorescence features of organic matter during WOMP co-composting has been carried out for the first time. The complexity of this type of compost is notably high. Specifically, while the three EEM-PARAFAC components, namely fulvic-like (C1), humic-like (C2) and protein-like substances (C3), were in agreement with other studies, it is worth noting that C3 exhibited multiple emission peaks associated with supramolecular interactions between proteins and polyphenols. Additionally, the results demonstrated that the HA fraction (classical procedure based on acid-base solubility of humic substances) was clearly enriched in the C2 component in mature composts, whereas the contribution of this component was underestimated in WEs. These humic-like substances not dissolved in WEs but present in compost can also play an important role upon soil application. Despite this drawback, WEs were found useful for rapidly assessing compost maturity as evidenced by the correlations with parameters of agronomic relevance.

CRedit authorship contribution statement

Marta P. Rueda: Writing – review & editing, Writing – original draft, Software, Methodology, Investigation, Formal analysis. **Ana Domínguez-Vidal:** Writing – review & editing, Writing – original draft, Supervision, Software, Methodology, Investigation, Formal analysis, Conceptualization. **María José Ayora-Cañada:** Writing – review & editing, Writing – original draft, Supervision, Software, Project administration, Methodology, Investigation, Funding acquisition, Formal analysis, Conceptualization. **Eulogio Llorent-Martínez:** Writing – review & editing, Writing – original draft, Methodology, Investigation, Formal analysis. **Víctor Aranda:** Writing – review & editing, Writing – original draft, Project administration, Methodology, Investigation, Funding acquisition, Conceptualization.

Declaration of Competing Interest

The authors declare that they have no known competing financial interests or personal relationships that could have appeared to influence the work reported in this paper.

Data Availability

Data will be made available on request.

Acknowledgements

This work has been financed by the research project PID2020-118673RB-I00 financed by MCIN/AEI/10.13039/501100011033 (Spanish Ministry of Science and Innovation). Technical and human support from the CICT-Universidad de Jaén is acknowledged (UJA, MINECO, Junta de Andalucía, FEDER). Marta P. Rueda also acknowledges the FPU22/00016 fellowship from the Spanish Ministry of Universities. Funding for open access charge: Universidad de Jaén.

Appendix A. Supporting information

Supplementary data associated with this article can be found in the online version at [doi:10.1016/j.eti.2024.103695](https://doi.org/10.1016/j.eti.2024.103695).

References

- Ait Baddi, G., Cegarra, J., Merlina, G., Revel, J.C., Hafidi, M., 2009. Qualitative and quantitative evolution of polyphenolic compounds during composting of an olive-mill waste-wheat straw mixture. *J. Hazard. Mater.* 165, 1119–1123. <https://doi.org/10.1016/j.jhazmat.2008.10.102>.
- Aran, D., Maul, A., Masfarau, J.F., 2008. A spectrophotometric measurement of soil cation exchange capacity based on cobalthexamine chloride absorbance. *Comptes Rendus. Geosci.* 340, 865–871. <https://doi.org/10.1016/J.CRTE.2008.07.015>.
- Artajo, L.S., Romero, M.P., Suárez, M., Motilva, M.J., 2007. Partition of phenolic compounds during the virgin olive oil industrial extraction process. *Eur. Food Res. Technol.* 225, 617–625. <https://doi.org/10.1007/S00217-006-0456-0>.
- BOE, 2017. Real Decreto 999/2017, de 24 de noviembre, por el que se modifica el Real Decreto 506/2013, de 28 de junio, sobre productos fertilizantes. *Boletín. Of. Del. Estado* 296, 119396–119450.
- Bro, R., Kiers, H.A.L., 2003. A new efficient method for determining the number of components in PARAFAC models. *J. Chemom.* 17, 274–286. <https://doi.org/10.1002/cem.801>.
- Canet, R., Pomares, F., Cabot, B., Chaves, C., Ferrer, E., Ribó, M., Albiach, M.R., 2008. Composting olive mill pomace and other residues from rural southeastern Spain. *Waste Manag.* 28, 2585–2592. <https://doi.org/10.1016/J.WASMAN.2007.11.015>.
- Cayuela, M.L., Mondini, C., Sánchez-Monedero, M.A., Roig, A., 2008. Chemical properties and hydrolytic enzyme activities for the characterisation of two-phase olive mill wastes composting. *Bioresour. Technol.* 99, 4255–4262. <https://doi.org/10.1016/J.BIORTECH.2007.08.057>.
- Droussi, Z., D’Orazio, V., Hafidi, M., Ouattmane, A., 2009. Elemental and spectroscopic characterization of humic-acid-like compounds during composting of olive mill by-products. *J. Hazard. Mater.* 163, 1289–1297. <https://doi.org/10.1016/J.JHAZMAT.2008.07.136>.
- Ferreira, C.S.S., Seifollahi-Aghmiuni, S., Destouni, G., Ghajarnia, N., Kalantari, Z., 2022. Soil degradation in the European Mediterranean region: Processes, status and consequences. *Sci. Total Environ.* 805, 150106. <https://doi.org/10.1016/J.SCITOTENV.2021.150106>.
- Fialho, L.L., da Silva, W.T.L., Milori, D.M.B.P., Simões, M.L., Martin-Neto, L., 2010. Characterization of organic matter from composting of different residues by physicochemical and spectroscopic methods. *Bioresour. Technol.* 101, 1927–1934. <https://doi.org/10.1016/J.BIORTECH.2009.10.039>.
- González-Cabrera, M., Domínguez-Vidal, A., Ayora-Cañada, M.J., 2018. Hyperspectral FTIR imaging of olive fruit for understanding ripening processes. *Postharvest Biol. Technol.* 145, 74–82. <https://doi.org/10.1016/J.POSTHARVIBIO.2018.06.008>.
- Guo, X., He, X., Zhang, H., Deng, Y., Chen, L., Jiang, J., 2012. Characterization of dissolved organic matter extracted from fermentation effluent of swine manure slurry using spectroscopic techniques and parallel factor analysis (PARAFAC). *Microchem. J.* 102, 115–122. <https://doi.org/10.1016/j.microc.2011.12.006>.
- He, X., Xi, B., Wei, Z., Guo, X., Li, M., An, D., Liu, H., 2011. Spectroscopic characterization of water extractable organic matter during composting of municipal solid waste. *Chemosphere* 82, 541–548. <https://doi.org/10.1016/j.chemosphere.2010.10.057>.
- Huang, J., Han, L., Huang, G., 2019. Characterization of digestate composting stability using fluorescence EEM spectroscopy combining with PARAFAC. *Waste Manag. Res.* 37, 486–494. <https://doi.org/10.1177/0734242X1982818>.
- Hu, J., Bi, J., Li, X., Wu, X., Wang, W., Yu, Q., 2023. Understanding the impact of pectin on browning of polyphenol oxidation system in thermal and storage processing. *Carbohydr. Polym.* 307, 120641. <https://doi.org/10.1016/J.CARBPOL.2023.120641>.
- Huo, S., Xi, B., Yu, H., He, L., Fan, S., Liu, H., 2008. Characteristics of dissolved organic matter (DOM) in leachate with different landfill ages. *J. Environ. Sci.* 20, 492–498. [https://doi.org/10.1016/S1001-0742\(08\)62085-9](https://doi.org/10.1016/S1001-0742(08)62085-9).
- Kellerman, A.M., Kothawala, D.N., Dittmar, T., Tranvik, L.J., 2015. Persistence of dissolved organic matter in lakes related to its molecular characteristics. *Nat. Geosci.* 8, 454–457. <https://doi.org/10.1038/NNGEO2440>.
- Liu, L., Song, C., Yan, Z., Li, F., 2009. Characterizing the release of different composition of dissolved organic matter in soil under acid rain leaching using three-dimensional excitation-emission matrix spectroscopy. *Chemosphere* 77, 15–21. <https://doi.org/10.1016/j.chemosphere.2009.06.026>.
- Lu, F., Chang, C.H., Lee, D.J., He, P.J., Shao, L.M., Su, A., 2009. Dissolved organic matter with multi-peak fluorophores in landfill leachate. *Chemosphere* 74, 575–582. <https://doi.org/10.1016/j.chemosphere.2008.09.060>.
- Mafra, I., Lanza, B., Reis, A., Marsílio, V., Campestre, C., De Angelis, M., Coimbra, M.A., 2001. Effect of ripening on texture, microstructure and cell wall polysaccharide composition of olive fruit (*Olea europaea*). *Physiol. Plant.* 111, 439–447. <https://doi.org/10.1034/J.1399-3054.2001.1110403.X>.
- Martín, A.P.S., Marhuenda-Egea, F.C., Bustamante, M.A., Curaqueo, G., 2023. Spectroscopy techniques for monitoring the composting process: a review. *Agronomy* 13, 2245. <https://doi.org/10.3390/AGRONOMY13092245>.
- Michailides, M., Christou, G., Akkratos, C.S., Tekerlekopoulou, A.G., Vayenas, D.V., 2011. Composting of olive leaves and pomace from a three-phase olive mill plant. *Int. Biodeterior. Biodegrad.* 65, 560–564. <https://doi.org/10.1016/j.ibiod.2011.02.007>.
- Milori, D.M.B.P., Galetti, H.V.A., Martin-Neto, L., Dieckow, J., González-Pérez, M., Bayer, C., Salton, J., 2006. Organic matter study of whole soil samples using laser-induced fluorescence spectroscopy. *Soil Sci. Soc. Am. J.* 70, 57–63. <https://doi.org/10.2136/sssaj2004.0270>.
- Murphy, K.R., Stedmon, C.A., Waite, T.D., Ruiz, G.M., 2008. Distinguishing between terrestrial and autochthonous organic matter sources in marine environments using fluorescence spectroscopy. *Mar. Chem.* 108, 40–58. <https://doi.org/10.1016/J.MARCHEM.2007.10.003>.
- Nahm, K.H., 2003. Evaluation of the nitrogen content in poultry manure. *Worlds Poultry Sci. J.* 59 (1), 77–88. <https://doi.org/10.1079/WPS20030004>.
- Nelson, D.W., Sommers, L.E., 1982. Total Carbon, Organic Carbon, and Organic Matter, in: Page, A.L., Miller, R.H., Kenney, D.R. (Eds.), *Methods of Soil Analysis: Part 2 Chemical and Microbiological Properties*. Agronomy Monographs, pp. 539–579. (<https://doi.org/10.2134/agronmonogr9.2.2ed.c29>).
- Pinho, I.A., Lopes, D.V., Martins, R.C., Quina, M.J., 2017. Phytotoxicity assessment of olive mill solid wastes and the influence of phenolic compounds. *Chemosphere* 185, 258–267. <https://doi.org/10.1016/J.CHEMOSPHERE.2017.07.002>.
- Plaza, C., Senesi, N., Brunetti, G., Mondelli, D., 2007. Evolution of the fulvic acid fractions during co-composting of olive oil mill wastewater sludge and tree cuttings. *Bioresour. Technol.* 98, 1964–1971. <https://doi.org/10.1016/j.biortech.2006.07.051>.
- Pontoni, L., Panico, A., Matanò, A., Van Hullebusch, E.D., Fabbriano, M., Esposito, G., Pirozzi, F., 2017. Modified sample preparation approach for the determination of the phenolic and humic-like substances in natural organic materials by the folin ciocalteu method. *J. Agric. Food Chem.* 65, 10666–10672. <https://doi.org/10.1021/acs.jafc.7b04942>.
- Richard, C., Guyot, G., Trubetskaya, O., Trubetskoy, O., Grigatti, M., Cavani, L., 2009. Fluorescence analysis of humic-like substances extracted from composts: influence of composting time and fractionation. *Environ. Chem. Lett.* 7, 61–65. <https://doi.org/10.1007/S10311-008-0136-3>.

- Roig, A., Cayuela, M.L., Sánchez-Monedero, M.A., 2006. An overview on olive mill wastes and their valorisation methods. *Waste Manag* 26, 960–969. <https://doi.org/10.1016/j.wasman.2005.07.024>.
- Rosario-Ortiz, F.L., Korak, J.A., 2017. Oversimplification of dissolved organic matter fluorescence analysis: potential pitfalls of current methods. *Environ. Sci. Technol.* 51, 759–761. <https://doi.org/10.1021/acs.est.6b06133>.
- Said-Pullicino, D., Erriquets, F.G., Gigliotti, G., 2007. Changes in the chemical characteristics of water-extractable organic matter during composting and their influence on compost stability and maturity. *Bioresour. Technol.* 98, 1822–1831. <https://doi.org/10.1016/J.BIORTECH.2006.06.018>.
- Santos, L.M. dos, Simões, M.L., de Melo, W.J., Martin-Neto, L., Pereira-Filho, E.R., 2010. Application of chemometric methods in the evaluation of chemical and spectroscopic data on organic matter from Oxisols in sewage sludge applications. *Geoderma* 155, 121–127. <https://doi.org/10.1016/j.geoderma.2009.12.006>.
- Stubbins, A., Lapierre, J.F., Berggren, M., Prairie, Y.T., Dittmar, T., Del Giorgio, P.A., 2014. What's in an EEM? Molecular signatures associated with dissolved organic fluorescence in boreal Canada. *Environ. Sci. Technol.* 48, 10598–10606. <https://doi.org/10.1021/es502086e>.
- Swift, R.S., 2018. Organic Matter Characterization, in: Sparks, D.L., Page, A.L., Helmke, R.H., Loeppert, P.N., Soltanpour, P.N., Tabatabai, M.A., Johnston, C.T., Summer, M.E. (Eds.), *Methods of Soil Analysis: Part 3 Chemical Methods*. SSSA Book Series, pp. 1011–1069. <https://doi.org/10.2136/sssabookser5.3.c35>.
- Tian, W., Li, L., Liu, F., Zhang, Z., Yu, G., Shen, Q., Shen, B., 2012. Assessment of the maturity and biological parameters of compost produced from dairy manure and rice chaff by excitation–emission matrix fluorescence spectroscopy. *Bioresour. Technol.* 110, 330–337. <https://doi.org/10.1016/J.BIORTECH.2012.01.067>.
- Wang, D., Mao, Y., Mai, L., Yu, Z., Lin, J., Li, Q., Yuan, J., Li, G., 2023. Insight into humification of mushroom residues under addition of Rich-N sources: comparing key molecular evolution processes using EEM-PARAFAC and 2D-FTIR-COS analysis. *J. Environ. Manag.* 329, 117079 <https://doi.org/10.1016/J.JENVMAN.2022.117079>.
- Wei, Z., Wang, X., Zhao, X., Xi, B., Wei, Y., Zhang, X., Zhao, Y., 2016. Fluorescence characteristics of molecular weight fractions of dissolved organic matter derived from composts. *Int. Biodeterior. Biodegrad.* 113, 187–194. <https://doi.org/10.1016/J.IBIOD.2016.03.010>.
- Wei, Z., Zhao, X., Zhu, C., Xi, B., Zhao, Y., Yu, X., 2014. Assessment of humification degree of dissolved organic matter from different composts using fluorescence spectroscopy technology. *Chemosphere* 95, 261–267. <https://doi.org/10.1016/J.CHEMOSPHERE.2013.08.087>.
- Wells, M.J.M., Hooper, J., Mullins, G.A., Bell, K.Y., 2022. Development of a fluorescence EEM-PARAFAC model for potable water reuse monitoring: Implications for inter-component protein–fulvic–humic interactions. *Sci. Total Environ.* 820, 153070 <https://doi.org/10.1016/J.SCITOTENV.2022.153070>.
- Wünsch, U.J., Murphy, K.R., Stedmon, C.A., 2017. The one-sample PARAFAC approach reveals molecular size distributions of fluorescent components in dissolved organic matter. *Environ. Sci. Technol.* 51, 11900–11908. <https://doi.org/10.1021/acs.est.7b03260>.
- Xu, Y., Bi, Z., Zhang, Y., Wu, H., Zhou, L., Zhang, H., 2022. Impact of wine grape pomace on humification performance and microbial dynamics during pig manure composting. *Bioresour. Technol.* 358, 127380 <https://doi.org/10.1016/J.BIORTECH.2022.127380>.
- Yang, L., Hur, J., Zhuang, W., 2015. Occurrence and behaviors of fluorescence EEM-PARAFAC components in drinking water and wastewater treatment systems and their applications: A review. *Environ. Sci. Pollut. Res.* 22, 6500–6510. <https://doi.org/10.1007/S11356-015-4214-3>.
- Yuan, D.H., An, Y.C., He, X.S., Yan, C.L., Jia, Y.P., Wang, H.T., He, L.S., 2018. Fluorescent characteristic and compositional change of dissolved organic matter and its effect on heavy metal distribution in composting leachates. *Environ. Sci. Pollut. Res.* 25, 18866–18878. <https://doi.org/10.1007/s11356-018-2067-2>.
- Yu, G.H., Luo, Y.H., Wu, M.J., Tang, Z., Liu, D.Y., Yang, X.M., Shen, Q.R., 2010. PARAFAC modeling of fluorescence excitation-emission spectra for rapid assessment of compost maturity. *Bioresour. Technol.* 101, 8244–8251. <https://doi.org/10.1016/j.biortech.2010.06.007>.
- Yu, M., He, X., Liu, J., Wang, Y., Xi, B., Li, D., Zhang, H., Yang, C., 2018. Characterization of isolated fractions of dissolved organic matter derived from municipal solid waste compost. *Sci. Total Environ.* 635, 275–283. <https://doi.org/10.1016/j.scitotenv.2018.04.140>.
- Zhang, S., Chen, Z., Wen, Q., Zheng, J., 2016. Assessing the stability in composting of penicillin mycelial dreg via parallel factor (PARAFAC) analysis of fluorescence excitation-emission matrix (EEM). *Chem. Eng. J.* 299, 167–176. <https://doi.org/10.1016/j.cej.2016.04.020>.
- Zhao, Y., Wei, Y., Zhang, Y., Wen, X., Xi, B., Zhao, X., Zhang, X., Wei, Z., 2017. Roles of composts in soil based on the assessment of humification degree of fulvic acids. *Ecol. Indic.* 72, 473–480. <https://doi.org/10.1016/J.ECOLIND.2016.08.051>.
- Zucconi, F., Pera, A., Forte, M., De Bertoldi, M., 1981. Evaluating toxicity of immature compost. *Biocycle* 22, 54–57.